



CT&F - Ciencia, Tecnología y Futuro

ISSN: 0122-5383

Instituto Colombiano del Petróleo (ICP) - ECOPETROL S.A.

Amado, Jonathan; Piedrahita, Carlos; Vera-Ciro, Carlos; Parra, Carlos  
SOLUTION OF A P AND S WAVE PROPAGATION  
MODEL USING HIGH PERFORMANCE COMPUTATION  
CT&F - Ciencia, Tecnología y Futuro, vol. 9, no. 1, 2019, pp. 119-130  
Instituto Colombiano del Petróleo (ICP) - ECOPETROL S.A.

DOI: <https://doi.org/10.29047/01225383.159>

Available in: <https://www.redalyc.org/articulo.oa?id=46570769012>

- How to cite
- Complete issue
- More information about this article
- Journal's webpage in redalyc.org

UDEM  redalyc.org

Scientific Information System Redalyc  
Network of Scientific Journals from Latin America and the Caribbean, Spain and  
Portugal

Project academic non-profit, developed under the open access initiative

#### ARTICLE INFO:

Received : May 01, 2018

Revised : August 29, 2018

Accepted : March 18, 2019

CT&F - Ciencia, Tecnología y Futuro Vol 9, Num 1 June 2019, pages 119 - 130

DOI : <https://doi.org/10.29047/01225383.159>

**ecopETROL**

[ctyf@ecopetrol.com.co](mailto:ctyf@ecopetrol.com.co)

# SPECIAL ISSUE ON SEISMIC IMAGING

## SOLUTION OF A P AND S WAVE PROPAGATION MODEL USING HIGH PERFORMANCE COMPUTATION

## SOLUCIÓN DE UN MODELO DE PROPAGACIÓN DE ONDAS P Y S, USANDO COMPUTACIÓN DE ALTO RENDIMIENTO

Amado, Jonathan<sup>a\*</sup>; Piedrahita, Carlos<sup>a</sup>; Vera-Ciro, Carlos<sup>a</sup>; Parra, Carlos<sup>b</sup>

### ABSTRACT

The propagation of seismic waves is affected by the type of transmission media. Therefore, it is necessary to solve a differential equation system in partial derivatives allowing for identification of waves propagating into an elastic media. This paper summarizes a research using a partial differential equation system representing the wave equation using the finite differences method to obtain the elastic media response, using an staggered grid. To prevent reflections in the computational regions, absorbent boundaries were used with the PML method. The implementation of the numerical scheme was made on two computational architectures (CPU and GPU) that share the same type of memory distribution. Finally, different code versions were created to take advantage of the architecture in the GPU memory, performing a detailed analysis of variables such as usage of bandwidth of the GPU internal memory, added to a version that is not limited by the internal memory in the graphic processing unit, but rather by the memory of the whole computational system.

### RESUMEN

La propagación de las ondas sísmicas se ven afectadas por el tipo de medio donde se transmiten. Por lo tanto se requiere solucionar un sistema de ecuaciones diferenciales en derivada parcial que permitan identificar las ondas que se propagan en el medio elástico. Este documento resume una investigación donde se usó un sistema de ecuaciones diferenciales parciales que representan la ecuación de onda utilizando el método de diferencias finitas para obtener la respuesta del medio elástico, usando una malla intercalada. Para evitar las reflexiones en las fronteras computacionales se utilizaron fronteras absorbentes con el método PML. La implementación del esquema numérico se realizó en dos arquitecturas de cómputo (CPU y GPU) que comparten el mismo tipo de distribución de memoria. Finalmente, se crearon diferentes versiones del código para aprovechar la arquitectura en la memoria de la GPU, se realiza un análisis detallado de variables como utilización y ancho de banda de la memoria interna de la GPU, además de una versión la cual no se ve limitada por la cantidad de memoria interna en la unidad de procesamiento gráfico sino por la cantidad de memoria que tiene todo el sistema de cómputo.

### KEYWORDS / PALABRAS CLAVE

Modelling | Elastic media | PML | GPU constant memory | GPU shared memory | Asynchronous copies and executions.  
Modelado | Medio elástico | PML | Memoria constante GPU | Memoria compartida GPU | Copias y ejecuciones no sincrónicas.

### AFFILIATION

<sup>a</sup>Universidad de Medellín, carrera 87 No 30-65 Medellín, Colombia

<sup>b</sup>Universidad de Pamplona, km 1 vía a Bucaramanga, Pamplona, Colombia

\*email: [jhonatanamadov@gmail.com](mailto:jhonatanamadov@gmail.com)

# 1 INTRODUCTION

The following work is intended to solve the bidimensional elastic wave equation in a high performance computational architecture; this process is commonly used in high cost computational algorithms such as RTM and FWI to infer, by means of seismic studies, the properties and location of the geological structures with hydrocarbon content in the subsurface. Essentially, seismic modelling is the construction of computational simulations to show the diverse reflection and refraction phenomena of energy in the subsurface. The key idea is to simulate the acquisition and reproduction of some synthetic records. This technique is a valuable tool for interpreting field seismograms and solution of seismic inversion algorithms.

Seismic imaging uses reflected energy to build an image of subsurface in order to investigate the underlying structure and stratigraphy. These can be compared with seismic records to review data such as layer thickness, type of rock, fault formation, fracturing and salt deposits. As these simulations demand numerous computational resources, it is necessary to use high performance computation that enables carrying out experiments and get results in the shortest time possible.

Similar work has been conducted in the area. Komatitsch, Erlebacher, Goddeke and Michea [1] discuss a formulation based on finite elements for the tridimensional wave propagation in an anisotropic media. Weiss and Shragge [2] developed wave field models in 2D and 3D in an anisotropic elastic media, resolving the equations with finite differences by using a regular grid, implemented in a massively parallel CUDA-based programming setting. Das, Chen and Hobson [3] in the study of seismic events, generated synthetic seismograms solving a tridimensional wave equation in elastic media using the pseudo-spectral method, parallelized in GPU units. The contribution of this work is the modelling of bidimensional wave propagation in elastic media, using a staggered grid to reduce the numerical dispersion. It is also implemented on a GPU-based structure and it is compared with the CPU implementation of several cores.

The document is organized as follows: the phenomena associated with the transmission of energy in P and S waves, together with the computational solution considerations are described in section two. Section three shows aspects related to the implementation while the results obtained are addressed in section four and the conclusions.

# 2. THEORETICAL FRAMEWORK

## PHENOMENOLOGY OF P AND S WAVES ENERGY TRANSMISSION

The energy of a seismic wave is transmitted in an isotropic elastic medium as two types of waves, those called P Waves, where the vibration of particles is polarized in the propagation direction and the S Waves, where the vibration of particles are polarized perpendicular to the wave propagation direction. The seismic modeling is a computational technique that allows to build simulations of energy reflection and refraction phenomena in the subsoil. An initial approach of the modelling for wave propagation in a medium is to consider the equation as if it were an acoustic medium; however, this approach does not consider the medium density variations, which is not the case in seismic data acquisition. To carry out the modeling process, the expressions for deformation in an elastic medium must be specified, to then arrive to the wave propagation formula in such medium.

The elastic dynamics has an energy conversion property when the wave front finds changes in the medium properties. This results in a longitudinal wave field (P) in the direction of the wave propagation direction, which modifies the volume of the medium by exerting compression, and a rotational wave field (S) which propagates transversal to the propagation direction. The interaction between these wave fields result in a dipolar behavior: the more P wave field amplitude the least S wave field amplitude and vice versa. To model these propagations, the internal forces of resistance to compression must be considered, which can be expressed through the stress tensor. At the same time, these forces give rise to acceleration and velocities in the medium, which are obtained synthetically through simulation or through seismic data acquisition. The ratios of velocities and stress tensor result in a differential equation system in partial derivate proposed by Virieux [4], and his solution

proposal through finite differences by Fornberg [5] result in an explicit numerical scheme shown in equations 1 to 5.

$$V_{x(i,k)}^{t+\frac{1}{2}} = V_{x(i,k)}^{t-\frac{1}{2}} + \frac{\Delta t}{\Delta h p_{(i,k)}} \left( T_{xx} \left( i+\frac{1}{2}, k \right) - T_{xx} \left( i-\frac{1}{2}, k \right) + T_{xz} \left( i, k+\frac{1}{2} \right) - T_{xz} \left( i, k-\frac{1}{2} \right) \right) \quad (1)$$

$$V_z \left( i+\frac{1}{2}, k+\frac{1}{2} \right) = V_z \left( i+\frac{1}{2}, k+\frac{1}{2} \right) + \frac{\Delta t}{\Delta h p_{\left( i+\frac{1}{2}, k+\frac{1}{2} \right)}} \left( T_{xx}^{t+1/2} \left( i, k+1 \right) - T_{xx}^{t+\frac{1}{2}} \left( i, k \right) + T_{xz}^{t+\frac{1}{2}} \left( i+1, k \right) - T_{xz}^{t+\frac{1}{2}} \left( i, k \right) \right) \quad (2)$$

$$T_{xx} \left( i+\frac{1}{2}, k \right) = T_{xx} \left( i+\frac{1}{2}, k \right) + \frac{\Delta t}{\Delta h} (\lambda + 2\mu) \left( i+\frac{1}{2}, k \right) \left( V_x^{t+\frac{1}{2}} \left( i+1, k \right) - V_x^{t+\frac{1}{2}} \left( i, k \right) \right) + \frac{\Delta t}{\Delta h} \lambda \left( i+\frac{1}{2}, k \right) \left( V_z^{t+\frac{1}{2}} \left( i, k+1 \right) - V_z^{t+\frac{1}{2}} \left( i, k \right) \right) \quad (3)$$

$$T_{zz} \left( i+\frac{1}{2}, k \right) = T_{zz} \left( i+\frac{1}{2}, k \right) + \frac{\Delta t}{\Delta h} (2\mu + \lambda) \left( i+\frac{1}{2}, k \right) \left( V_z^{t+\frac{1}{2}} \left( i, k+1 \right) - V_z^{t+\frac{1}{2}} \left( i, k \right) \right) + \frac{\Delta t}{\Delta h} \lambda \left( i+\frac{1}{2}, k \right) \left( V_x^{t+\frac{1}{2}} \left( i, k+1 \right) - V_x^{t+\frac{1}{2}} \left( i, k \right) \right) \quad (4)$$

$$T_{xz} \left( i, k + \frac{1}{2} \right)^{t+1} = T_{xz} \left( i, k + \frac{1}{2} \right)^t + \frac{\Delta t}{\Delta h} \mu \left( i, k + \frac{1}{2} \right) \left( V_x^{t+1/2} - V_x^{t+\frac{1}{2}} + V_z^{t+\frac{1}{2}} - V_z^{t+\frac{1}{2}} \right) \quad (5)$$

Where  $V_x$  and  $V_z$  are the velocity fields in the horizontal and depth axis, respectively.  $T_{xx}$ ,  $T_{zz}$  and  $T_{xz}$  are the tensions on planes  $xx$ ,  $zz$  and  $xz$  respectively. The  $t$  variable is the time integration index,  $i$  is the coordinate index on axis  $x$  and  $k$  is the coordinate index on axis  $z$ . The grid steps over time and on spatial axis  $x$  and  $z$  are  $\Delta t$  and  $\Delta h$  respectively. The  $\mu$  y  $\lambda$  values correspond to Lamé coefficients. The stability condition is more restrictive due to the presence of shearing velocity  $V_z$  given by formula 1 as proposed by Barnberger, Chavent and Lailly[6], considering that  $\Delta x = \Delta z$ .

When these equations are modelled and both wave fields are obtained and these get close to an interface given by the change of medium, part of the energy is reflected and the other one is refracted. When a P wave field is reflected, there will be a new P wave field and an S wave field. This is also the case with refracted energy. This phenomenon is known as conversion of the P-S energy and is shown in Figure 1.

In order to prove this computational scheme, a solution of the acoustic and elastic equation is presented in a three-layer heterogeneous model whose dimensions are 4 km distance and 2.4 km depth for axis  $x$  and  $y$ , respectively. The experimental parameters are shown in Table 1.

**Table 1.** Parameters of a three-layer heterogeneous medium for testing the reflection and refraction in the acoustic and elastic media.

Layer	Vp (m/s)	Vs (m/s)	Density (kg/m <sup>3</sup> )
1	1028	607	1590
2	1753	553	1028
3	2131	1209	1860

Considering that the source is located within the model and on the surface ( $x = 2\text{km}$ ,  $y = 0\text{km}$ ), all events occurred during the simulation of 1.7s are registered, rendering the results shown in Figure 2b for the simulation in the acoustic medium and the results are shown in Figures 3a and 3c for the simulation in the elastic medium. With respect to the acoustic simulation, the expected response is the direct wave and to additional reflections from the 2 interfaces for the three-layer model. As regards the elastic simulation in both registers  $V_x$  and  $V_z$ , there are more than 2 reflections due to the Energy conversion.

## CONSIDERATIONS ABOUT THE COMPUTATIONAL SOLUTION.

### THE PERTURBATION SOURCE

As regards the perturbation source, the Ormsby filter is used, which consists in a trapezoidal zero-phase wavelet for its frequency response. In the seismic exploration area, this type of wavelet is useful as it is similar to the acquisitions with vibrator trucks, as these allow for observing low or high frequency noise while the wave energy dissipates as it propagates in length and depth. The frequencies in this case are  $f_1$ ,  $f_2$ ,  $f_3$ ,  $f_4$ : 5, 10, 60 and 80Hz respectively, where  $f_1$  is the low cutoff frequency,  $f_2$  is the low-passing frequency,  $f_3$  is the high-passing frequency and, finally,  $f_4$  is the high cutoff frequency. Figure 3a shows the response of a homogeneous medium to an Ormsby source in an acoustic medium, and Figure 3b and 3c represent the solution of the wave equation in an elastic medium. Two perturbations are identified in these figures, one of them represented by a P wave velocity field, and the second one is the medium response given by the shear-velocity. Lastly, Figure 3d and 3e show the response in the time domain and in the frequency domain, respectively.

### MANAGEMENT OF BOUNDARY CONDITIONS

The absorbing boundary conditions are desirable to eliminate artificial reflections produced when the energy propagation simulation reaches the limits of the implementation matrix, which size is finite. In theory, the wave fronts propagate toward infinite while energy dissipates, but actually the mesh where the simulation takes place has logical limits, which generate false reflections. There are several proposals to solve this problem. One proposal

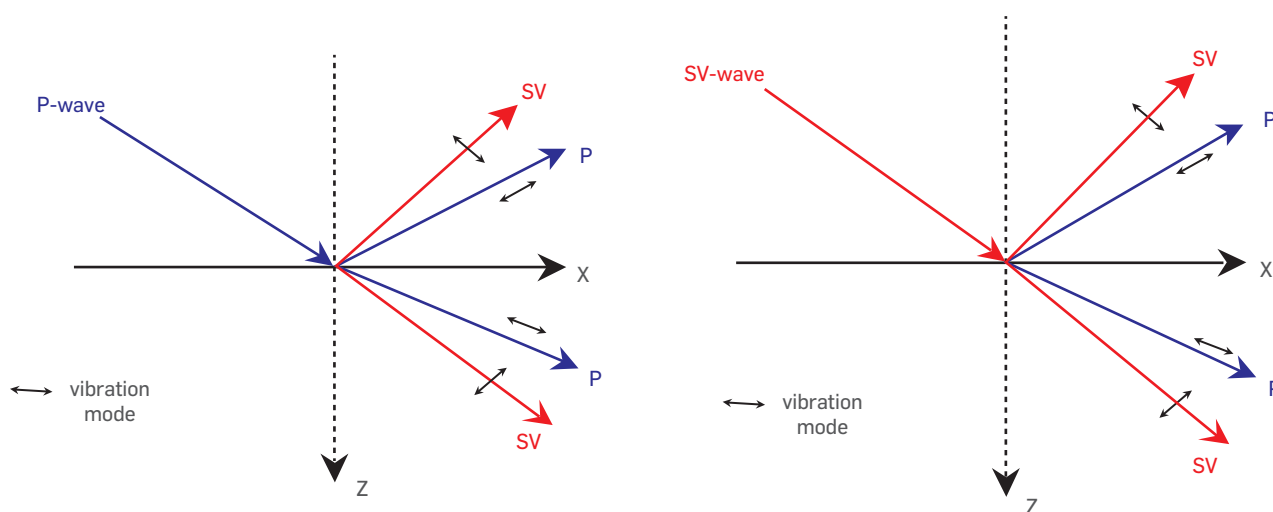


**Figure 1.** Reflection and Refraction phenomena of P and S waves. Left: P waves, right: S waves.

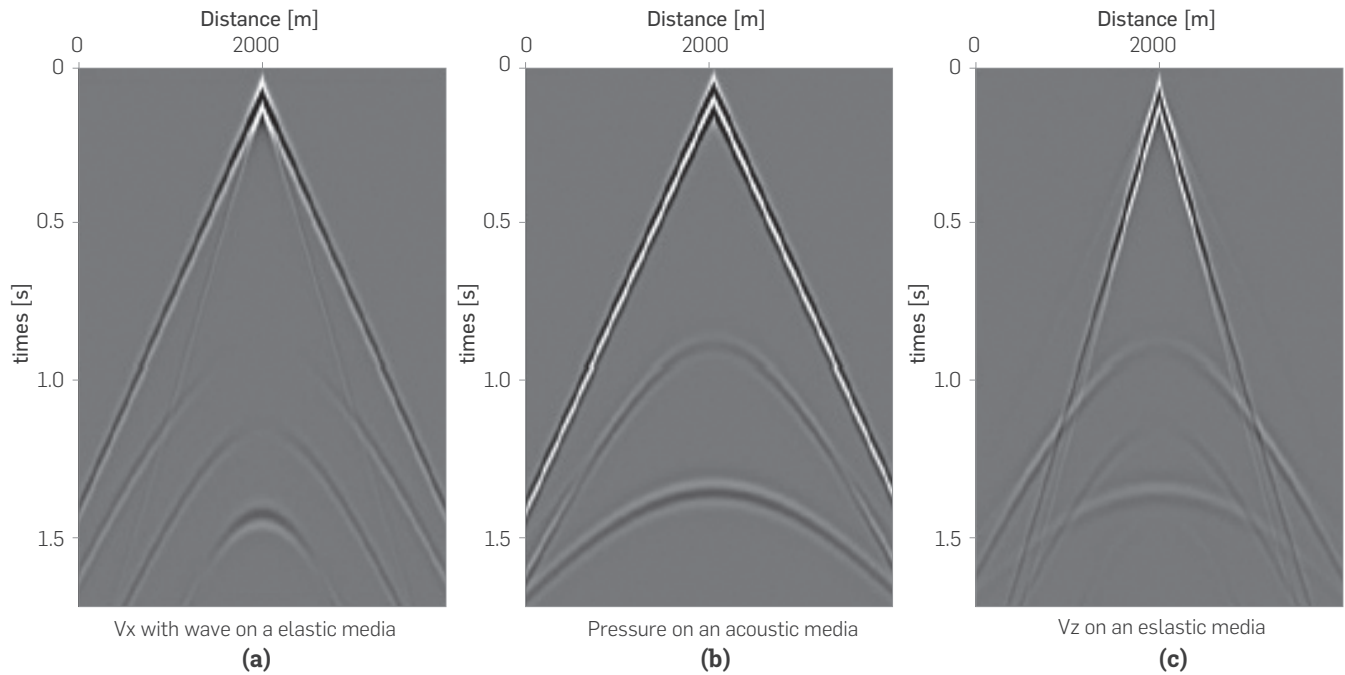


**Figure 2.** Records for a three-layer model with data presented in table 1. (a) Vx con onda en medio elástico (b) Presión en medio acústico (c) Vz en medio elástico

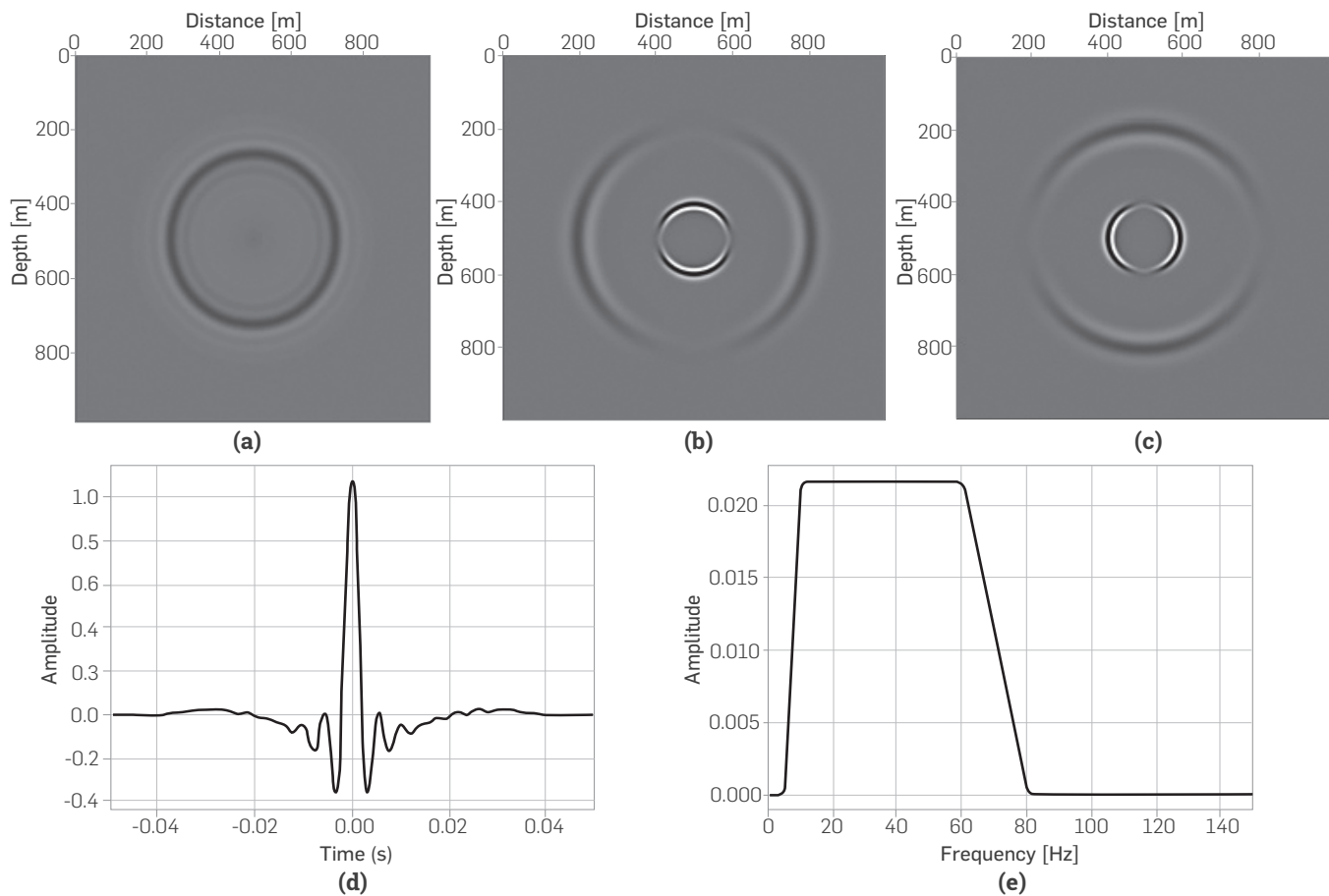


**Figure 3.** Simulation of the response of the medium in pressure and velocities of an Ormsby wavelet. (a) Response of pressure field to an Ormsby wavelet in an acoustic homogeneous medium (b) Response of the Vx field to an Ormsby wavelet in an elastic homogeneous medium (c) Response of the Vz field to an Ormsby wavelet in an elastic homogeneous medium (d) Response of the Ormsby Wavelet [5-10-60-80]Hz in function of the time (e) Frequency response of the Ormsby Wavelet [5-10-60-80]Hz



that has rendered good results if that of the Perfectly Matched Layer (PML) by Berenger[7], whose initial implementations were done with electromagnetic simulations. In the continuous limit it has been confirmed that the PML has no reflections, regardless of the incidence angle and the frequency established by Zeng and Liu [8] and there are no instability problems related to the models where the ratio  $V_s/V_p$  is less than 0.5 as proposed by Mahrer [9] and Stacey [10]. The PML region is located near the computational limit as shown in **Figure 4**. Following a Cartesian plane, the 2D elastic wave equation can be expressed as a first order differential equation system in terms of velocity and stresses in the particles and its implementation can be formulated with a simple variable division procedure in the spatial domain, where one component is tangential to the field and the other is orthogonal.

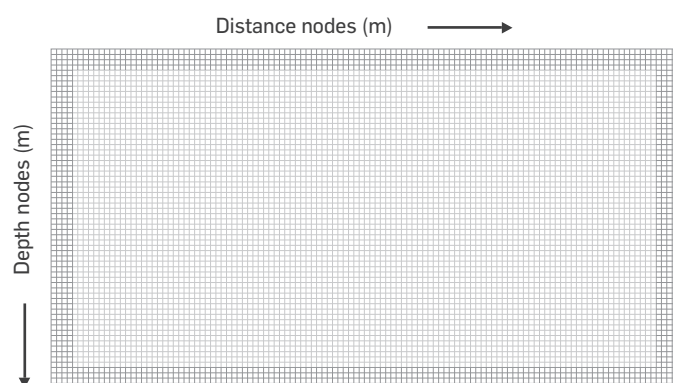


**Figure 4.** Matrix scheme near the computational limits. The dark region is an area of the grid where false reflections are attenuated

To prove the numerical validity of the PML, the experiment shown in **Figures 5a-5h** was performed. A source is located in the position (800,800)[m] and all events in the position (300,800) [m] are registered, which is marked on the guide intersection lines on **Figures 5a-5c** and **5e-5g**. The parameters used in the PML are 20 points and an amortization coefficient  $R=0.0001$  showing the following results in **Figure 5**.

It is noted that when using the PML there is no wave amplitude reflected and, therefore, there will be no reflections due to computational boundaries.

#### BOUNDARY INSTABILITY SOLUTION.

When dividing the velocity and deformation components on tangential and orthogonal elements to apply the PML, there is one specific case in which this form of wave attenuation shows instability and that is when there are shear-velocity components  $V_s=0$  and  $V_s>0$ , which is common when reproducing offshore seismic acquisitions. The next experiment is a simple geological model where the upper layer is water and the lower layer is a solid. Such instability can be observed in the experiment shown in **Figures 6a** to **6f**.

To solve this instability issue, it was proposed to use a gaussian filter only on the shear velocity values within the PML zone, so that in places where the transition  $V_s=0$  (water) and  $V_s>0$  exists, it would be as smooth as possible. Keeping this in mind, the same experiment was reproduced, obtaining the results shown in **Figures 7a** to **7f**.

### 3. EXPERIMENTAL DEVELOPMENT.

Nearly all new processors work on the development of computational architecture based on central processing units (hereinafter CPU), where the processor received instructions from the memory that are subsequently decoded to finally execute the instruction and store the result again in the memory.

The distributed computation, commonly called cluster computing is a good way to solve large applications demanding high computational costs. This notion consists in taking a given number of computers and connecting them in a network with the potential of enhancing several times the computational performance to solve the application. However, it should be taken into account that the network velocity is a limiting factor.

The architecture in a modern graphic processing unit (GPU) is no different than a multi-node scheme. The GPU has a finite number of multiprocessors (SMs) that are very similar to the cores in a CPU. A modern GPU is connected to a computation system by means of a PCI port that is much faster than a network connection. This way it would be possible to have better performance, without being limited by the transmission of the results.

The notion behind better performance in GPU is that these processing units comprise a processor array (SM), each with N cores. The more SMs in the GPU, the more tasks processed simultaneously. In each SM there are several SP (units that have an array of a series of processing cores and special function units). Each SM has access to a set of records that have the same velocity than an SP unit, where each SP has a shared memory, which is accessible for each SM.

#### COMPUTATION SYSTEM USED

In order to compare the efficiency of computation architectures, some implementation tests were performed on different architectures. With respect to CPU tests, these were performed in the next processing node belonging to the research group of Connectivity and Processing of Signals (CPS) of Universidad Industrial de Santander.

The programming environment used was CUDA (Compute Unified Device Architecture), which is an extension for programming languages such as C, C++, FORTRAN, Python and others; it supports the graphic processing units to execute applications created in those languages. The CUDA language extensions follow a heterogeneous programming concept. The foregoing means that to execute applications in a graphic processing unit, the main program must be launched by the processor and then the functions that are to be executed in parallel will be launched in the GPU. These functions are executed in graphic processing units.

**Table 2.** Used CPUs's features.

Testing equipment	
CPU tests	GPU tests
Processor: 2x intel Xeon E5-2670 V3 @ 2.3GHz; 24 physical cores. Cache memory L1 24x32KB, L2 24x256KB, L3 30MB.	Processor: 1x intel core i7 4790 @ 3.6GHz; 4 physical cores & underclock @2.3GHz. Cache memory L1 4x32KB, L2 4x256KB L3 8MB
RAM Memory: 64GB DDR3	RAM Memory: 32GB DDR3
No GPU Device	GPU GTX980ti GDDR5 6GB
USD Cost: 15000	USD Cost: 2200

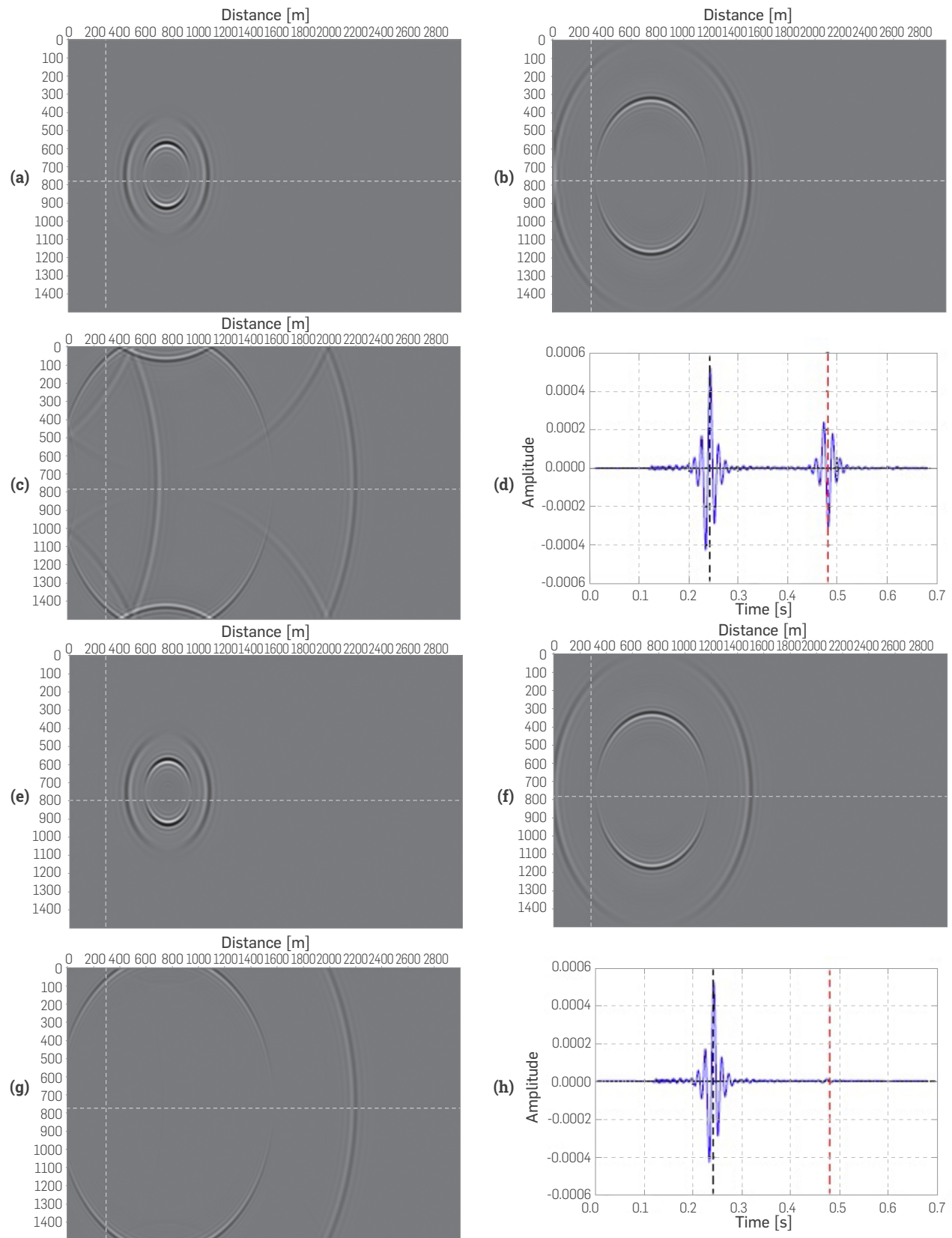


**Figure 5.** Experiments to test behavior in the grid boundary using the PML. (a) Simulation time 0.2[s] (b) Simulation time 0.3[s] (c) Simulation time 0.5[s] (d) Record of incident and reflected wave by the boundary, without using PML. (e) Simulation Time 0.2[s] (f) Simulation Time 0.3[s] (g) Simulation Time 0.5[s] (h) Record of incident and reflected wave by the boundary, using PML.

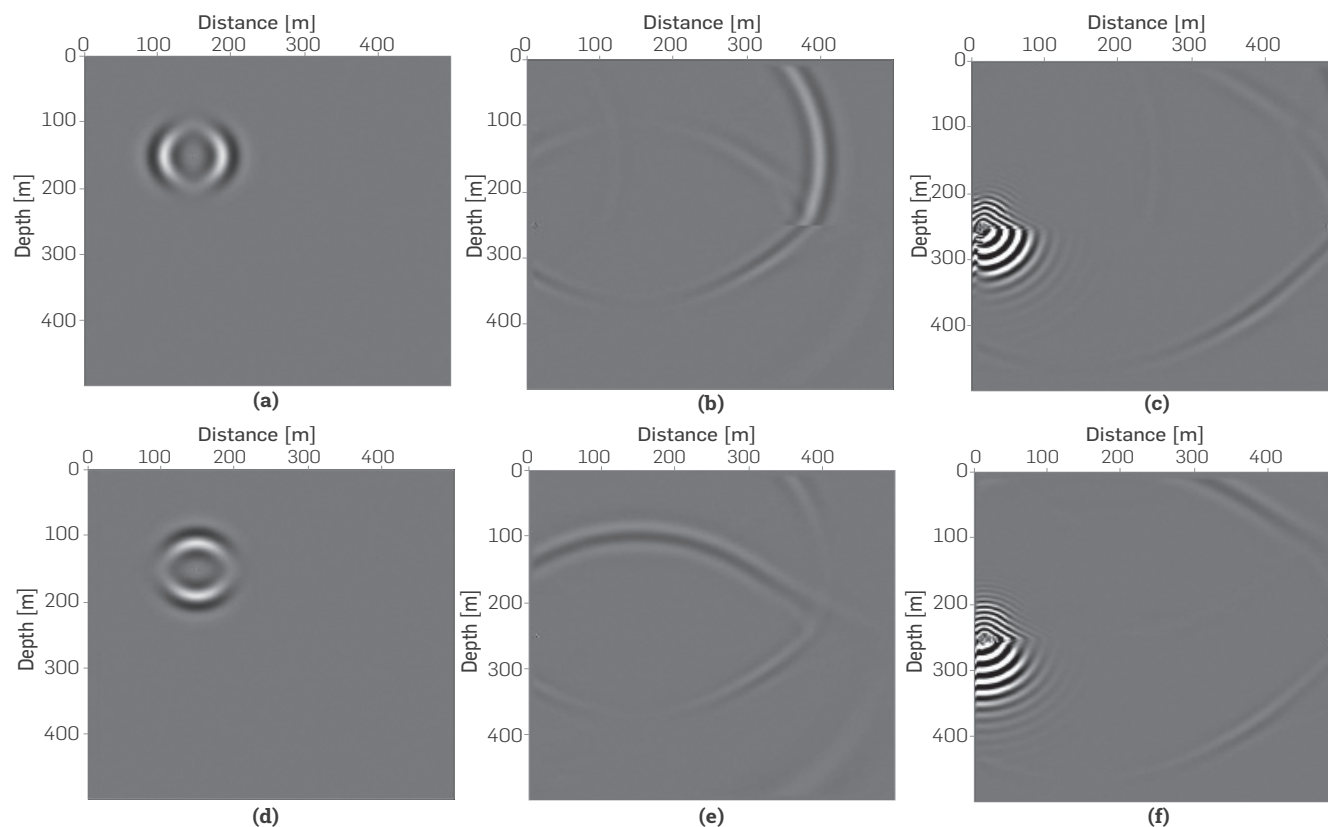


**Figure 6.** (a) Vx field at  $t=0.04[s]$  (b) Vx field at  $t=0.1[s]$  (c) Vx field at  $t=0.2[s]$  (d) Vz field at  $t=0.04[s]$  (e) Field Vz at  $t=0.1$  (f) Vz field at  $t=0.2[s]$

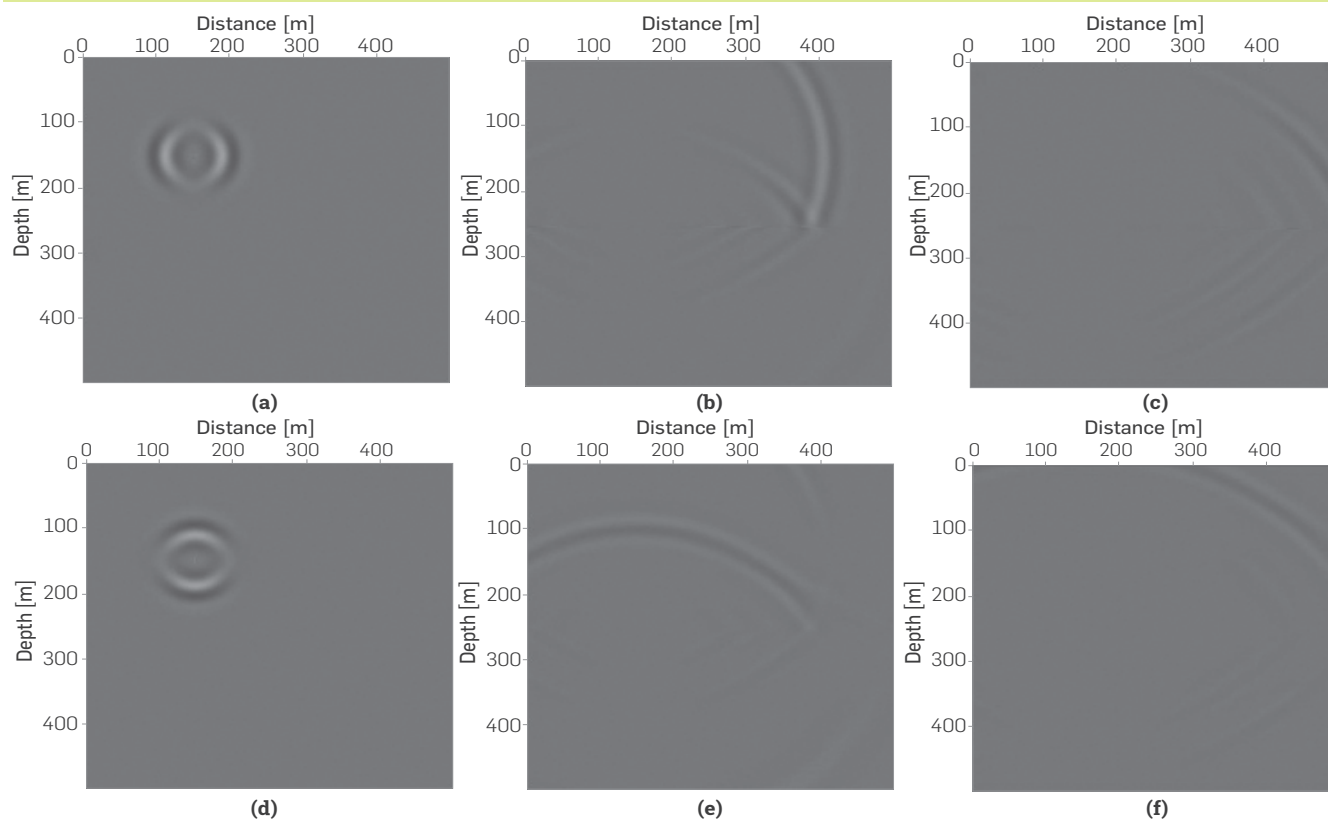


**Figure 7.** (a) Vx field at  $t=0.04[s]$  (b) Vx field at  $t=0.1[s]$  (c) Vx field at  $t=0.2[s]$  (d) Vz field at  $t=0.04[s]$  (e) Vz field at  $t=0.1[s]$  (f) Vz field at  $t=0.2[s]$



## IMPLEMENTATION IN CPU AND GPU COMPUTATIONAL ARCHITECTURE.

For implementation in all CPU cores, the OpenMP programming extensions were used, which enables dividing the programming cycles (for) in the number of threads of the processor. This programming model is based on shared memory systems. This means that each thread can access the whole memory reserved for the application, carry out any operation and write thereon. It is, therefore, fundamental to make a distinction between private and shared variables.

The Marmousi elastic model will be used, as standard, in all tests, which dimensions are 13601 x 2801. This model has a spatial interval  $\Delta h$  of 1m and due to the small memory of the GPU, the idea is to simulate only 1.1 seconds of a seismic acquisition. In general, a seismic acquisition implies 4 to 6 seconds recording and, therefore, the use of asynchronous executions and memory copies is proposed further below in order to fully simulate a seismic acquisition in the GPU, with the limit not being the memory of the GPU but the RAM memory of the whole computation system to thus obtain faster executions. All operations, both in CPU and GPU, were done with double precision arithmetic.

There are two basic forms of dividing the work load in a CPU that is, using static or dynamic distributions. The experiment was conducted trying both forms, having chosen the dynamic distribution as it is closer to the ideal performance, as can be seen in Figure 8.

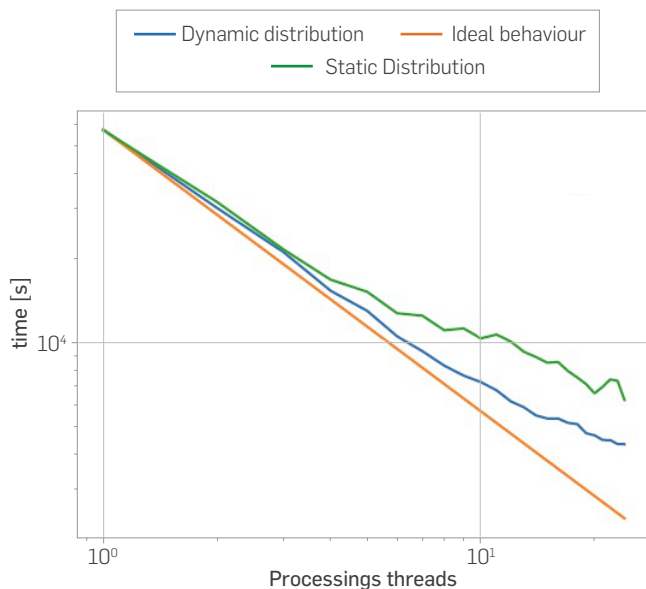


**Figure 8.** Solution of the elastic wave equation in the Marmousi model, with a simulation time of 1.1[s] through static and dynamic distribution. Time using dynamic distribution with 1 core  $t_1=57023[s]$ , Time using dynamic distribution with 24 cores  $t_{24}=4325[s]$ .

With respect to the implementation in the GPU, 3 versions were issued. The first one is a simple coding where all variables are stored in the global memory of the GPU. The second one uses the constant memory and the shared memory of the GPU to accelerate even more the calculations, and a third version called (Zero-Copy) where even using the shared and constant memories, asynchronous copies

between the GPU memory and the CPU memory were made in order to simulate in the GPU a full acquisition without being restricted by its small memory.

Equal to the code execution in the CPU, the time to be simulated is 1.1[s] and for each version the intent is to change the block size to determine the size with the shortest execution time. The sizes of the blocks used were 2x2, 4x4, 8x8, 16x16. The test using 32x32 thread blocks was possible only by using the global memory (version 1 of the code), as the GPU architecture has restrictions related to the use of the shared memory with blocks containing 1024 threads or more.

The best performance is obtained by using 16x16 blocks, regardless of the copies being synchronous or asynchronous, as observed in Figure 9, even though the additional time of the kernel (core) with asynchronous copies is approximately 20[s] more.

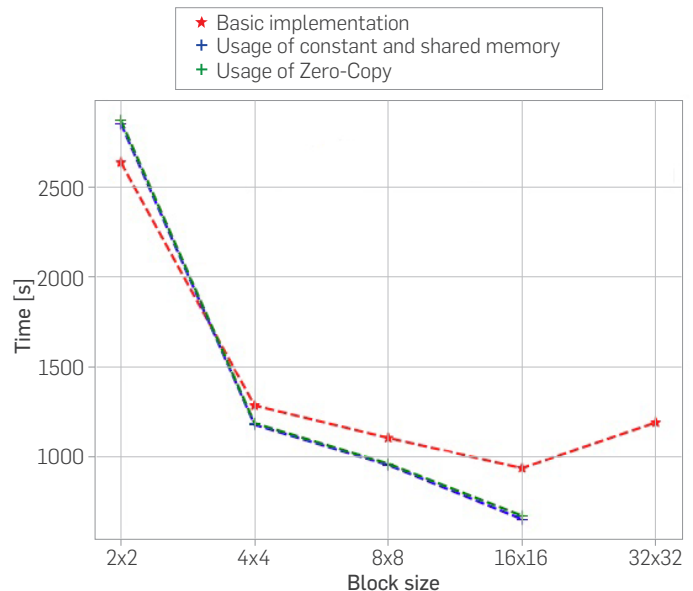


**Figure 9.** Equation solution of the elastic wave in the Marmousi model, using a GPU in function of the block size. Time of the zero copy version using a block 2x2  $t_{zp2x2}=2871[s]$ . Time of the zero copy version using a block 16x16  $t_{zp16x16}=670[s]$ .

## 4. RESULTS ANALYSIS

### EXECUTION LIMITED BY LATENCY OR MEMORY

After knowing the size of the ideal block to obtain the shortest execution time, it is assessed if this type of kernel is limited by latency or by memory. A latency problem is that the instruction to be executed by the thread has so many operations to carry out that it is limited by the clock velocity of the thousands of cores in a GPU. On the contrary, a memory problem issued is how dependent is the instruction on uploading all values from the memory to then perform the respective operation.

Ideally there should be a homogeneous performance and as high as possible between the operation functions and the memory transactions. Using the Nvidia Visual Profiler (NVVP) [11] tool, it is possible to evaluate the overall performance of the application

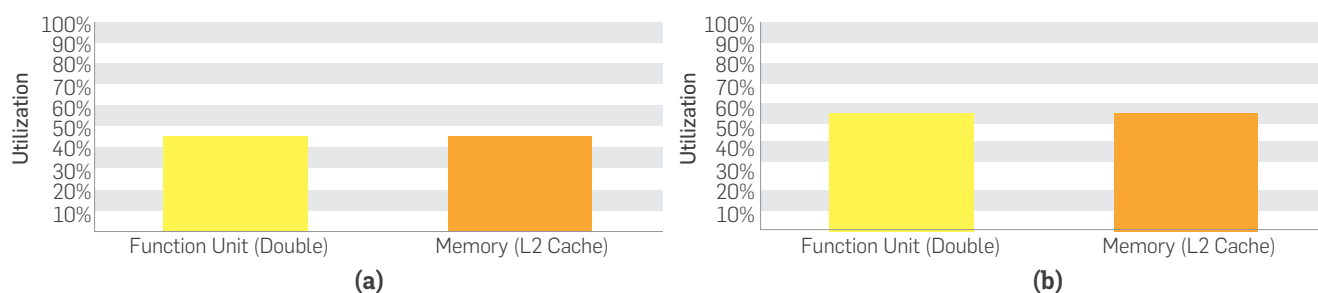


**Figure 10.** (a) Percentage of use of computation functions and GDDR5 memory using version 1 (global memory) (b) Percentage of use of computation functions and GDDR5 memory using version 3 (zero copy + const\_mem + shared\_mem)

execution in the GPU. To such end, version 1 of the code is compared vs. version 3, where the shared memory and the constant memory in the kernel are used, as this helps to a faster uploading of the values, thus increasing the velocity of the execution. When using this type of memory, in practice the preloading of values for processing the elastic wave equation improves by nearly 10 per cent points (55%)

the response of the GPU with respect to latency and memory transfer.

A more detailed analysis of memory performance can be observed by analyzing the throughput of each implementation as observed in Figures 10a, 10b, 11a and 11b.

	Transactions	Bandwidth	Utilization	
<b>Shared Memory</b>				
Shared Loads	0	0 B/s		
Shared Stores	0	0 B/s		
Shared Total	0	0 B/s		
<b>L2 Cache</b>				
Reads	12632923	459.643 GB/s		
Writes	2100232	76.416 GB/s		
<b>Total</b>	<b>14733155</b>	<b>536.059 GB/s</b>		
<b>Unified Cache</b>				
Local loads	0	0 B/s		
Local Stores	0	0 B/s		
Global loads	21028900	459.613 GB/s		
Global Stores	2100226	76.416 GB/s		
Texture Reads	9492552	345.382 GB/s		
Unified Total	32621678	881.41 GB/s		
			Idlie	low Medium High Max

	Transactions	Bandwidth	Utilization	
<b>Shared Memory</b>				
Shared Loads	525954	129.224 GB/s		
Shared Stores	598818	147.126 GB/s		
Shared Total	1124772	276.35 GB/s		
<b>L2 Cache</b>				
Reads	6319638	388.174 GB/s		
Writes	1050119	64.502 GB/s		
<b>Total</b>	<b>7369757</b>	<b>452.676 GB/s</b>		
<b>Unified Cache</b>				
Local loads	0	0 B/s		
Local Stores	0	0 B/s		
Global loads	10521137	388.128 GB/s		
Global Stores	1050113	64.502 GB/s		
Tecture Reads	4748850	291.691 GB/s		
Unified Total	16320100	744.321 GB/s		
			Idlie	low Medium High Max

**Figure 11.** (a) Throughput analysis for version 1 of de code (global memory)  
(b) Throughput analysis for version 3 of de code (zero copy + const\_mem + shared\_mem))

## USAGE OF THE GPU

The usage factor of the GPU can be obtained by evaluating the kernel with the NVVP [CUDA, 2017] tool, in addition to other significant variables for assessing the kernel performance such as:

- Active blocks
- Active threads
- Active warps

To visualize kernel results, a comparison was made between basic implementation in a GPU and implementation using asynchronous copies with shared and constant memories, which responses are shown in **Figures 12a** and **12b**. As can be observed in the figure, a detailed use of the various memory hierarchies provided by this GPU architecture can increase by nearly 20 per cent points the Occupancy variable, which shows how busy the GPU is calculating with active threads. Having values in the shared memory enables having more active blocks, as these will not have to wait for obtaining values

from the global memory. Another aspect to analyze is the behavior of records with respect to active threads. When feeding the shared memory, the records upload the additional values; therefore, it is ideal when these are integer numbers and multiples of the number of threads that exist in a warp. When using the shared memory and uploading the additional values for calculating the eighth order stencil, this translates in the record access to the threads being as aligned as possible. This ratio can also be seen in **Figures 12c** and **12d** under the SM occupancy heading.

## OPERATIONS BY TIME UNIT

One of the most relevant measures in the high performance computation setting is the number of operations required by a certain computation unit to fully complete a task. This unit is known as flops. The last analysis proposed is to record operations by time unit required by the CPU to carry out the task and the necessary operations in each of the 3 implementations in the GPU, resulting on that shown in **Figure 13**.

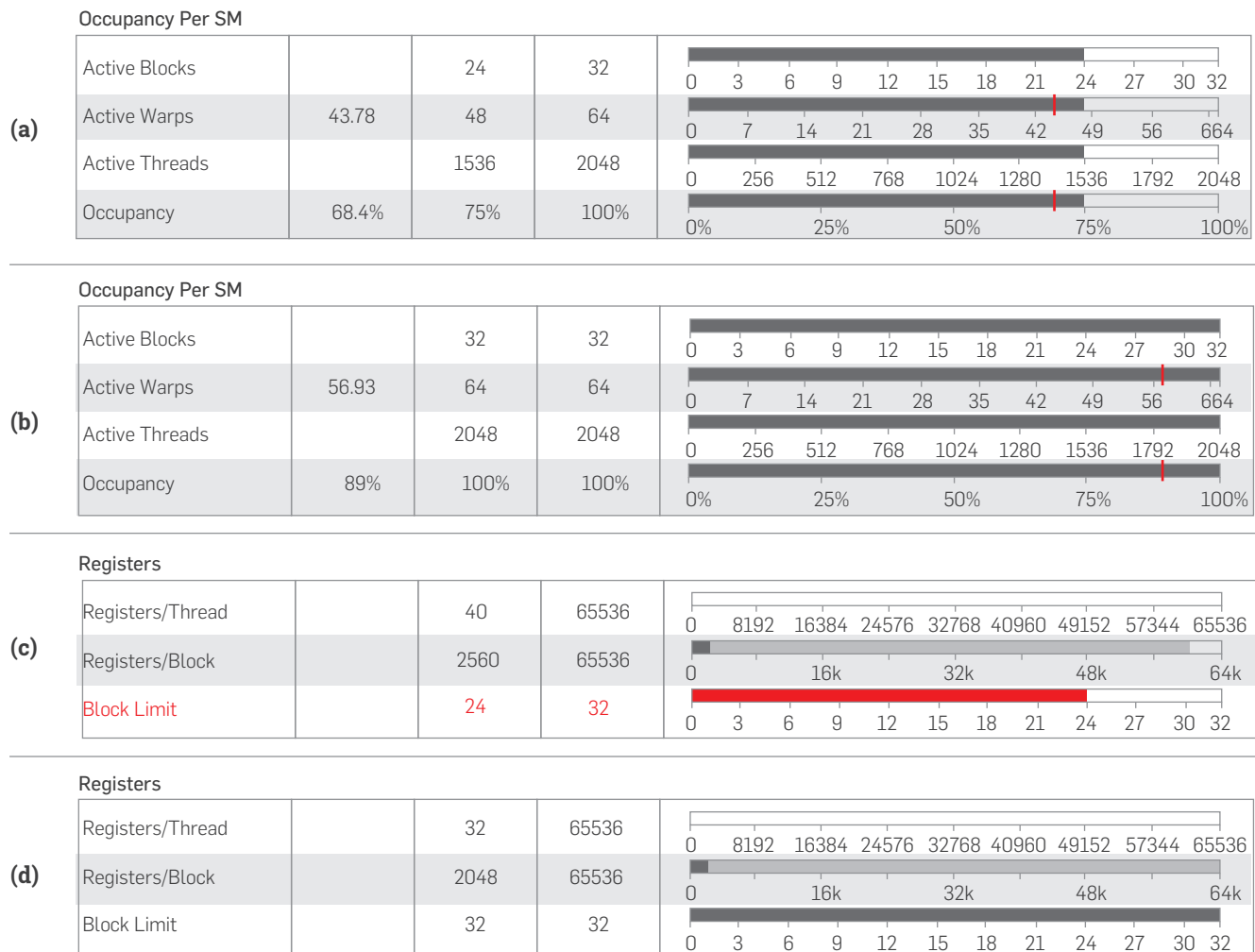


**Figure 12.** (a) Variable Occupancy per SM (utilization per multiprocessor) in the implementation of the code using the global memory only (b) Variable Occupancy per SM (utilization per multiprocessor) in the implementation of the code using the zero-copy + mem const + mem shared. (c) Usage of records per thread, per block and block limit using the global memory (d) Usage of records per thread, per block and block limit using zero-copy + mem cons + mem shared.

It is evident that using a GPU to solve this type of simulations is much more efficient than using a CPU, but if the performance is to be even better, the code that was developed should be restructured to use concurrent kernels.

## CONCLUSIONS

The bidimensional wave equation in isotropic medium was solved by means of finite differences in the temporary domain in two computation architectures, with programming shared memory applications. When working out this equation, the stability of the various test models was evident.

Furthermore, the Ormsby wavelet set in the tests is a type of signal commonly used in synthetic experiments, as it enables

obtaining response of the medium in a wide range of frequencies.

A comparison was made with respect to the execution time between two different processing architectures, such as a CPU and a GPU. As regards the CPU, its processing resources and memory were used as much as possible, using the OPENMP application programming interface to use all the processing cores. Several simulation experiments were performed for comparing their performance as related to execution times and floating point operations. It is concluded that the execution of the modelled process is more efficient when using the implementation in GPU (use of zero-copy with shared memory and constant memory) vs. the implementation in a 24-core CPU, as it is almost 12 times faster. Thus, a GPU is an alternative to carry out fast and efficient calculations.

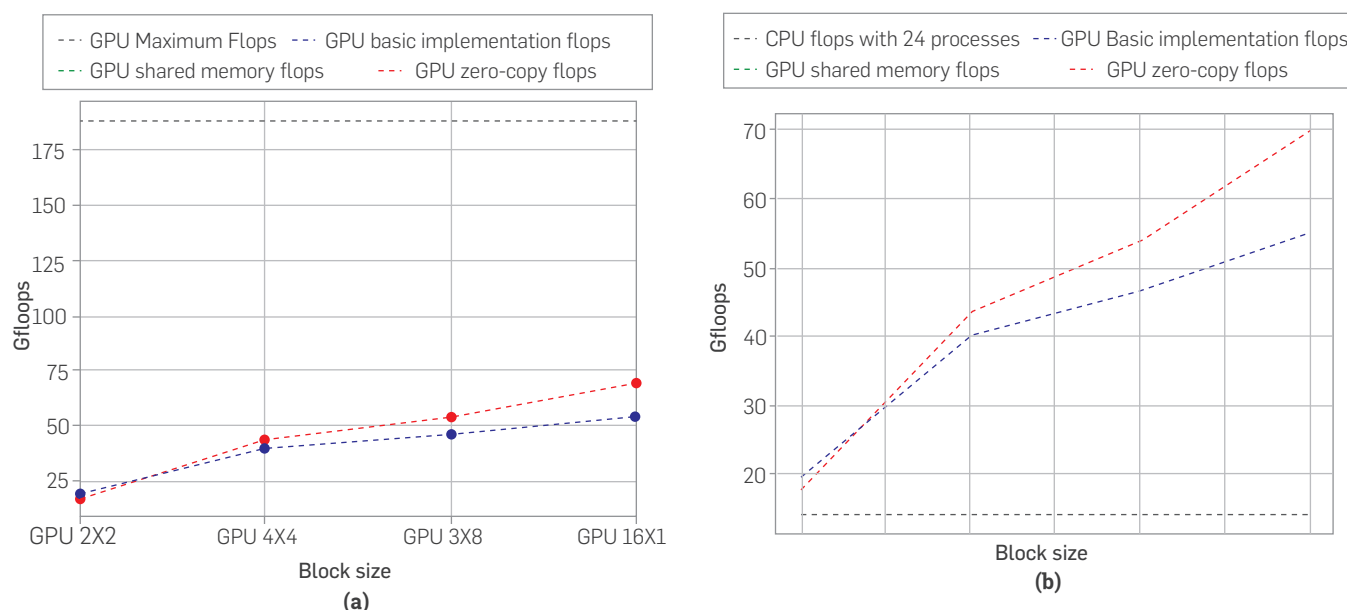


**Figure 13.** Comparison in accordance with the floating point operations criteria.

## ACKNOWLEDGEMENTS

This work was supported by Empresa Colombiana de Petróleos - Ecopetrol and Colciencias, as part of the research project based on agreement 0266 of invitation 531 of 2013. The authors are also grateful for the support offered by the CPS group of Universidad Industrial de Santander and the Computational Science group of Universidad de Pamplona.

## REFERENCES

- [1] Komatitsch, D., Erlebacher, G., Goddeke, D., and Michea, D. (2010). High-order finite-element seismic wave propagation modeling with MPI on a large CPU cluster. *Journal of Computational Physics*, (229), pp. (7692-7714). doi: 10.1016/j.jcp.2010.06.024
- [2] Weiss, R. and Shragge, J. (2013). Solving 3D anisotropic elastic wave equations on parallel GPU devices. *Geophysics*. Volume 78, pp. 1-9. Doi: 10.1190/geo2012-0063.1
- [3] Das, S., Chen, X., and Hobson, M. (2017). Fast GPU-based seismogram simulation from microseismic events in marine environments using heterogeneous velocity models. *IEEE transactions on computational imaging* V 3:1 2, pp. 316-329. doi: 10.1109/TCI.2017.2654127
- [4] Virieux, J. (1986). A p-sv wave propagation in heterogeneous media: Velocity-stress finite difference method. *Geophysics*. Volume 51, pp. 899 - 904. doi: 10.1190/1.1442147
- [5] Fornberg, B. (1988). Generation of finite difference formulas on arbitrarily spaced grids. *Mathematics of Computation*. Volume 51, pp. 699-706. doi: 10.1090/S0025-5718-1988-0935077-0
- [6] Bamberger, A., Chavent, G., and Lailly, P. (2006). Étude de schémas numériques de l'élastodynamique linéaire. Technical report, INRIA. <https://hal.inria.fr/inria-00076520/document>



[7] Berenger (1994). A perfectly matched layer for the absorption of electromagnetic waves. *Journal of Computational Geophysics*. Volume 114 pp. 185-200. doi: 10.1006/jcph.1994.1159

[8] Zeng and Liu (2001). The application of the perfectly matched layer in numerical modeling of wave propagation in poroelastic media. *Geophysics*. Volume 66, pp. 1258-1266. doi: 10.1190/1.1487073

[9] Mahrer (1986). An empirical study of instability and improvement of absorbing boundary conditions for elastic wave equation. *Geophysics*. Volume 51 pp. 1499 - 1507. doi: 10.1190/1.1442198

[10] Stacey (1988). Improved transparent boundary formulations for the elastic wave equation. *Bulletin of Seismological Society of America*. Vol. 78, pp. 2080 - 2097. doi:.

[11] NVIDIA Corporation, (2017). *CUDA NVIDIA visual profiler*. <https://developer.nvidia.com/nvidia-visual-profiler>

DE TODOS,  
PARA TODOS

